In-situ process monitoring in deep-drawing of paper using partially transparent tools

CÉDRIC BRUNK AND PETER GROCHE

ABSTRACT: The production of three-dimensionally formed packaging from paper by deep drawing usually leads to the occurrence of wrinkles, which result from the high tangential compressive stresses in the flange area and the limited flowability of the material. Wrinkles, although mostly tolerated in industry, end in both a reduced visual appearance and a reduction in usability for packaging, as with, for example, when gas-tightness is required.

Previous research efforts have been limited to determining the wrinkle distribution after completion of forming and removal of the formed part. Consequently, the possibility of understanding the sequence of formation of individual wrinkles in the inhomogeneous material is lost. To remedy this situation, a method for local in-situ process monitoring is presented.

Using a transparent die and an industrial camera, the flange area can be observed during the forming process. An image processing algorithm is applied to analyze the local development of the deep drawing process from the continuously recorded image data.

The method described can be used to analyze the draw-in behavior and wrinkle formation locally and continuously over the drawing depth. The blank holder force influences the draw-in and the wrinkle pattern both locally and throughout the drawing process. A more precise understanding of the wrinkle formation will allow for more efficient process control in the future.

Application: This paper presents findings on wrinkle formation during deep drawing of paper that were gained through an innovative approach that provides direct insight into the forming zone. Image-based algorithms can be used to analyze material displacement and wrinkle formation over the process progression.

The reduction of single-use plastic-based packaging is being driven by legislation and society, leading to a high demand for sustainable alternatives to fossil-based materials. As consumer willingness to pay more for sustainable packaging has decreased since 2021 and remains at a surplus of about 6%, cost-effective processes are critical for widespread adoption [1]. Paper-based packaging with high volumes of goods can be produced by several processes, such as fiber molding, folding, and wrapping. Fiber molding offers high geometrical freedom, but results in a rough surface structure. Additionally, the complex and, therefore, expensive tools and the high energy consumption are further disadvantages. Folding and wrapping paper blanks are two common variants of two-dimensional forming that occurs along a straight line. As a result, geometric complexity is limited or multiple sequential forming steps are required to produce complex packaging.

An alternative is using three-dimensional forming techniques such as active media-based forming, press forming, or deep drawing, all of which are adopted from sheet metal forming. These processes enable a high degree of geometric freedom while still providing adequate surface quality. In deep drawing, a blank is positioned and clamped between a drawing die and a blank holder, as shown in **Fig. 1a–1b**. By means of the applied forming force, the punch pushes the blank in the drawing gap between the

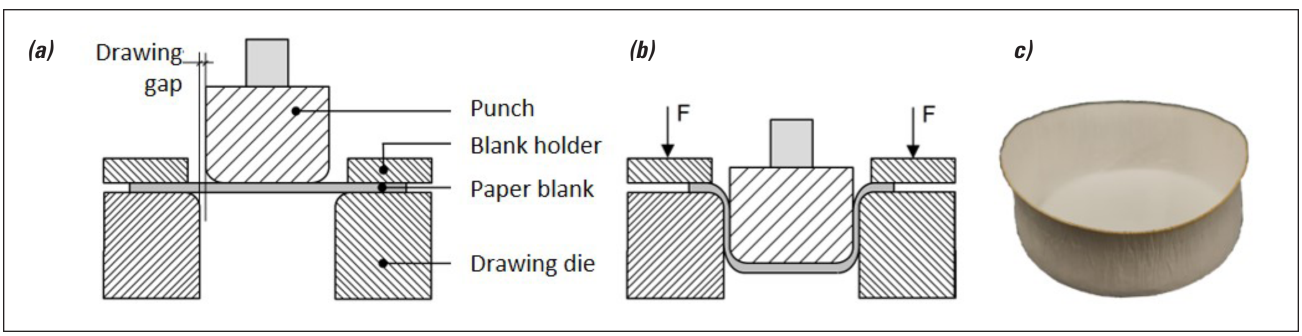

1. Deep drawing of paper board: (a) initial and (b) final process steps adopted from [2]; and (c) deep drawn part.

punch and the drawing die. Due to the reduction of the circumference of the blank and the resulting excess material, tangential compressive stresses occur in the remaining material between the blank holder and the die, the so-called flange area. As in all sliding blank-forming methods, the limited yield of the paper leads to excessive wrinkling in the flange [3]. In deep drawing, the wrinkles are further compressed in the drawing gap, as in Fig. 1c. The blank holder force influences the formation of wrinkles and is therefore the most relevant process parameter [4]. Hauptmann et al. divide the deformation mechanisms during the deep drawing of paper into three phases [5]. In the first phase, the deformation of the fiber network takes place without wrinkling, while in the second phase, the deformation is caused by wrinkles and shear deformation. In the third phase, the material is restructured, and the wrinkled areas are compressed. During wrinkling of materials with multi-ply layered structure, the delamination is the primary mechanism of deformation under in-plane compression, leading to nonuniform load distribution and wrinkle formation [6].

Besides wrinkling, rupture is a process failure influenced by material and process parameters such as the blank holder force and drawing gap clearance, as well as the die and punch radii. After removal of the formed part, springback occurs due to elastic strain components, which are usually nonuniform due to the anisotropic mechanical properties of industrially fabricated paper.

Variants such as press forming use a mold with inclined walls (angle greater than 90° from the bottom area). Due to the longer free-forming length without a blank holder, wrinkle control is reduced. Therefore, the wrinkle appearance is often predetermined by the creasing of the blank before forming [7].

In active media-based forming, the punch is replaced by pressurized air or a fluid. With well-chosen process parameters, wrinkle-free parts, as required for gas-tight sealing, can be produced using only elongation of the material. This fixed blank forming method leads to relatively smooth surfaces [3]. A downside is the limited drawing depth due to the paper's limited maximum strain [8].

Deep drawing represents an economically viable option for producing high-volume parts with high geometrical freedom and good surface quality. However, anisotropic springback and excessive wrinkling pose challenges regarding functional sealing and marketing-relevant printing, limiting its use. It is therefore the subject of ongoing research.

Hauptmann et al. [9] describe the influence of the blank holder force on springback behavior and wrinkling. They show the number of wrinkles over the drawing depth for different blank holder force profiles, using a so-called "optimized" trajectory determined over maximum bearable force. The wrinkles are counted at different heights at drawn parts after removal from the forming machine. This shows that there is an initial drawing height of a few millimeters where the excess material is compressed within the material structure without forming wrinkles.

The forming process and wrinkle formation are also subject to numerical modeling. Wallmeier et al. describe an explicit finite element model with which the material behavior is simulated up to wrinkle formation and is suitable for investigating influencing factors up to first wrinkle formation [10]. The numerical modeling of wrinkle formation is studied by Linvill et al., in which a one-dimensional model with perfectly plastic hinges was applied to the wrinkle formation in the deep drawing of paper [11]. The influence of moisture is also analyzed in numerical simulations. A global increase in moisture shows an increase in the maximum drawing depth, while localized moistening has a positive effect on wrinkle distribution [12].

Several approaches are described to quantify the wrinkles. In addition to manual counting using pure eyesight or a microscope, some automated detection systems are described in the literature. The most advanced development of an automated flange and wrinkle detection system is presented by Müller et al. [13] as a series of improvements to a system initially described by Wallmeier et al. [14]. Hereby, the visual quality of a deep-drawn part positioned on an LED matrix with a diffuser plate is analyzed using an industrial camera and image processing. The contrast of the wrinkle structure in backlighting is increased compared to a dome light setting and allows the detection of wrinkles in the flange area of parts after removal. In image processing, the outer contour of the drawn part is detected using value thresholding. The wrinkle detection is based on the cross-correlation of the recorded images with a template of an ideal wrinkle structure, which was initially described by Müller et al. [15]. The most recent, but more simplified, approach is described by Leng et al., who detect wrinkles in specimens also imaged in transmitted light using a brightness threshold of the transmitted light, taking into account shape correction due to anisotropic springback where necessary [16].

A common drawback of all the approaches described is that the wrinkles can only be recorded after completion and removal from the die. This means that information about the chronological sequence in which the wrinkles are created is lost. Furthermore, it is no longer possible to intervene in the process to specifically influence the material flow and wrinkle formation. As a basis for closed-loop controls and due to their high information content about the product quality, the sensor-based detection of flange draw-in and wrinkling during the process is of great interest in deep drawing. Various common sensor concepts are summarized by Allwood et al. [17]. In particular, a distinction can be made between systems that measure at one or more discrete points in the flange area and systems that measure at the outer edge. Measurements are taken tactile or contactless (e.g., using optical sensors), which are implemented at eight positions in the die [18].

All of the methods used to date have the common dis-

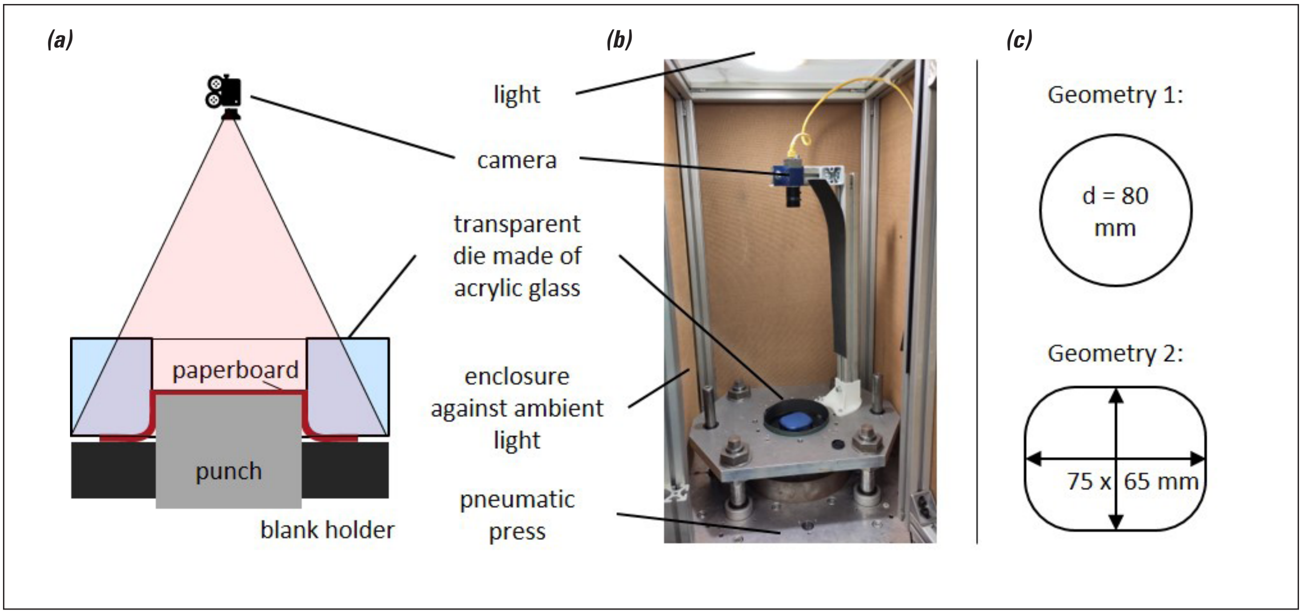

2. (a) Schematic of deep drawing setup with transparent die and camera; (b) realization of pneumatic press; and (c) forming geometries used for study.

advantage that the material flow can only be detected at discrete points and changing the position is usually time- and resource-consuming. Partially transparent tools allow insights into regions of interest and open possibilities for image-based analysis, but they have found little application so far. Due to the high forces involved in metal forming and cold forming in particular, high-cost single crystals such as diamond or quartz refined glass are used for this purpose. These are used as inserts in forming tools and enable local optical process data acquisition [19,20].

This paper describes a setup for in-situ process monitoring using transparent tool parts. A transparent die and an industrial camera allow material flow and wrinkle formation to be observed locally and continuously over the drawing depth. This enables in-depth analysis of the material flow and wrinkle formation and paves the way for subsequent local process control.

METHODS

Deep drawing setup

The deep drawing setup used on a pneumatic press is shown in **Fig. 2a–2b**, consisting of a transparent die and an industrial camera. The transparent die is made of acrylic glass machined by cutting tools from a solid plate. The high availability of plates up to 50-mm thick and the low cost compared to other transparent materials, such as glass or minerals like sapphire or diamond, make the use of thermoplastics ideal for low process forces.

The punch and blank holder are produced by additive manufacturing using black-colored polylactic acid (PLA) filament for the blank holder to ensure high contrast against the white paperboard. Above the die, a gray-image industrial camera with a resolution of 5 megapixels (MP) and up to 22 frames/second (fps) is mounted with a 16-mm objective. The recording setup is housed within an enclosure and lighted from above to guarantee a reproducible lighting situation.

For this study, two different geometries were used for the punch and die, as shown in Fig. 2c. While in the first geometry the influence of the anisotropic material behavior becomes easily apparent, the second geometry leads to varying degrees of excess material in the flange due to the straight and convex parts. The trademarked TrayForma bleached tray board from Stora Enso was used in this study with a grammage of 350 g/m² [21]. The bleached virgin fiber paperboard consists of three layers and was stored at 95% relative humidity and 20°C to increase the moisture content to about 15% for increased formability. By storing at higher humidities, the elongation increased from 1.5% in the machine direction (MD) and 4.5% in the cross direction (CD) at standard conditions (23°C, 50% relative humidity) to 2.6% (MD) and 6.2% (CD). At the same time, the tensile strength decreased from 59 N/mm² (MD) and 27 N/mm² (CD) to 45 N/mm² (MD) and 23 N/mm² (CD).

Processing algorithm

The camera stream is recorded with a sampling rate of 20 fps during the forming process, which has a duration of about 1 s, and is analyzed after completion using the evaluation algorithm. Since the algorithm will be used in real time during the process in later studies, special attention is paid to the short computing time. The algorithm, which is applied to every single frame of the sequence and is shown in **Fig. 3**, is implemented in MATLAB 2021 (Mathworks; Natick, MA, USA) and uses packages from the image processing toolbox (MathWorks) [22].

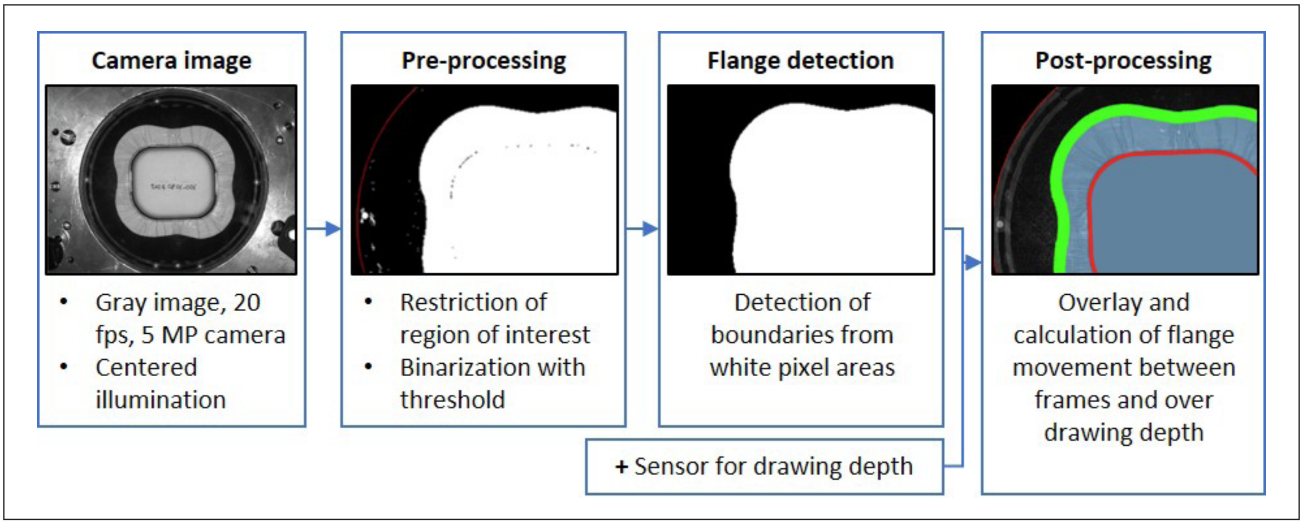

3. Image processing algorithm for flange detection.

First, the gray images are cropped with a static mask to obtain the region of interest without the mounting of the die and other irrelevant system components. A binarization is then performed to distinguish the white paper blank from the black surface of the blank holder. In the binarized image, small objects in the blank holder result from impurities or reflections, represented by isolated clusters of white pixels. They are removed by applying a morphological area opening operation "bwareaopen" based on a limit value chosen to be less than 5% of the total image size. The holes, represented by isolated black pixels, within the sample area are then filled using the "imfill" operation. The result of the operations is a binary image in which the area of the paper blank is represented by white pixels. In the next step, the "bwboundaries" operation is used to identify the contour of the blank. The method traces the exterior boundaries of objects in the binary image and is based on the Moore-Neighbor tracing algorithm. A comparison with expected values or the change between successive frames can be carried out to validate correct recognition. The overall processing time for one frame sums up to 37 ms without further optimization such as multithreading on a GPU.

In the final step, the algorithm's results are visualized, and the frame-by-frame change in the contour is determined. The forming press is equipped with a displacement sensor that allows the assignment of a corresponding drawing depth to each frame of the video, which is used for subsequent evaluation. Due to the concentric arrangement of the camera and the die, the contour of the die can also be integrated as a static shape for visualization and calculation of the remaining flange length. The calculated flange data is useful for transforming into polar coordinates, which is also implemented in the post-processing step.

In addition to detecting the flange draw-in, the material flow within the flange area can be observed and analyzed using digital image correlation (DIC). To do so, a speckle pattern with a point size of 0.52 mm was printed on the paperboard before deep-drawing. The recorded images are then fed into an industrial DIC software (GOM Correlate) to calculate the local displacements in the flange.

RESULTS

Flange draw-in

This section describes the flange draw-in results for both geometries. **Figure 4a** shows an image of the initial state with a drawing depth of 0 mm and a more advanced frame during the process with a corresponding drawing depth of 15 mm for the round geometry. The MD of the paperboard is aligned horizontally, as shown by the arrow. The flange, detected by the method described previously, is overlaid with a blue solid thick line. Additionally, radial distances from the center point towards the flange at angles of multiples of 45° are shown in colored solid and dashed lines. The radial distances from the center point to the flange are shown in Fig. 4b for several drawing depths over the circumference with corresponding angles of the multiples of 45°. As can be seen from the diagram, the radius at the initial state (top line) corresponds to a nearly horizontal line, with slight deviations due to inaccurate alignment when inserting the sample. With further increase of the drawing depth, the radius decreases, showing anisotropic draw-in. In MD, the decrease over the first 5 mm drawing depth is significantly higher than in CD, which can be explained by the anisotropic behavior of the material. Under the same load, paperboard shows less elongation in MD than in CD, which leads to the formation of an oval-shaped flange when forming with a round geometry, as more material has to be drawn-in in MD instead of straining. This observation is consistent with previous experience that round deep drawing geometries result in an oval part [12]. At a greater drawing depth, the differences in CD and MD remain nearly constant. This is caused by reducing the radius over the circumference at a nearly constant rate. At a high drawing depth, the detected radius appears more irregular, which

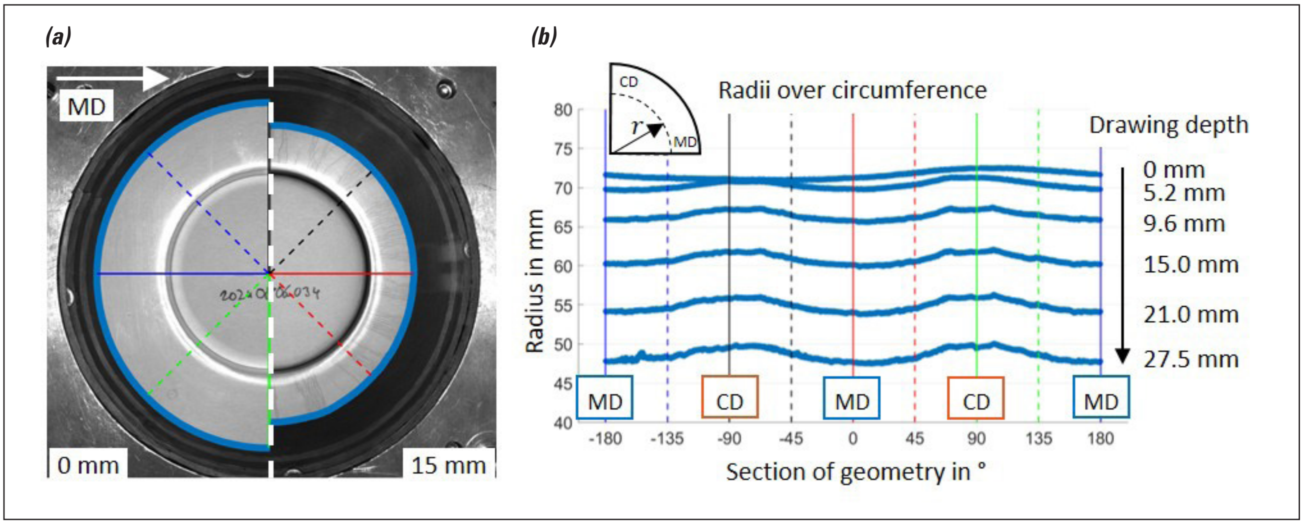

4. (a) Videoframe with detected flange at beginning and advanced state, and (b) radii over circumference for several drawing depths for round geometry.

can be explained by the occurrence of wrinkles and was previously described by Vishtal et al. [23].

The reduction of the radii compared to the initial radius at the beginning of the process is shown in **Fig. 5a** over the drawing depth. Here, the mean value of the radii in MD (0° and ± 180°) and CD (± 90°) and the associated standard deviation are calculated.

With this visualization, it becomes apparent that the draw-in does not start immediately at the beginning of the deep drawing process, but at a drawing depth of a few millimeters. Before that, the deepening happens only due to the elongation of the material and without material flow in the flange area. At a drawing depth of about 2 mm, the draw-in starts in MD, whereas in CD, the first draw-in can be observed at about 4 mm drawing depth. This is in accordance with the findings in Fig. 4 and can be explained by the anisotropic behavior of the paperboard, which becomes apparent immediately at the start of the process.

The blank holder force as the main process parameter of the deep drawing process also influences the draw-in behavior, as can be seen in Fig. 5b, where the draw-in at a drawing depth of 25 mm is compared for different blank holder forces. With higher force, the draw-in decreases, which can be explained by increased strain, as described by Müller et al. for different drawing parameters [4].

In **Fig. 6**, the same results are shown for the rectangular deep drawing geometry. On the left side, an image of the initial state with a drawing depth of 0 mm and a more advanced frame during the process with a corresponding drawing depth of 19.8 mm is presented. Over the drawing process, a nonuniformity in the draw-in can be detected, resulting in a bone-shaped final geometry with longer flange in curved segments compared to straight segments. The mean and standard deviation of all four curved and straight segments are visualized over the drawing depth. Again, a drawing depth of about 3 mm can be reached without a draw-in due to the elongation of the paper. After beginning of the draw-in, a difference in flange length between straight and curved seg-

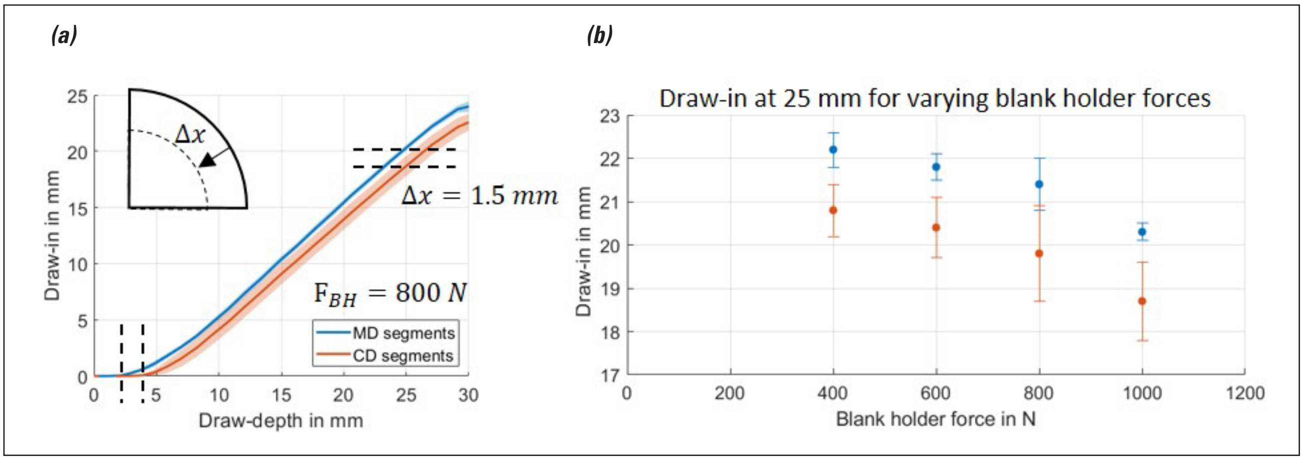

5. (a) Draw-in of machine direction (MD) and cross direction (CD) segments over drawing depth for fixed blank holder force (F_{BH}), and (b) difference in draw-in for varying F_{BH} for round geometry.

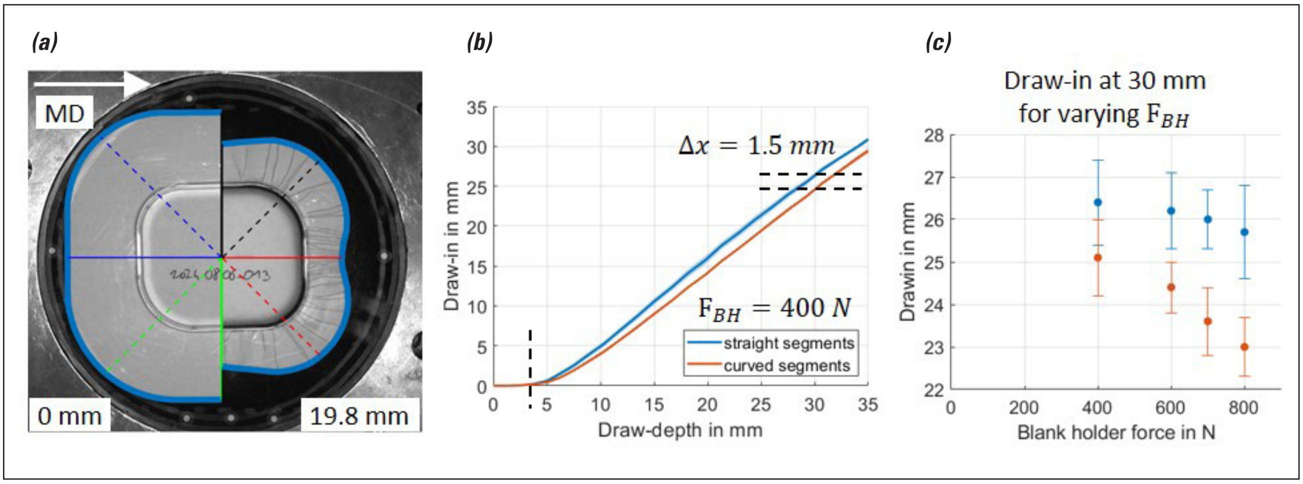

6. (a) Video frame with detected flange at beginning and advanced state; (b) draw-in of straight and curved segments over draw-depth for fixed blank holder force (F_{BH}); and (c) difference in draw-in for varying F_{BH}.

ments is recognized. This effect can be explained by the anisotropic material properties and the multi-axial stress in the curved segments. In addition to the radial tensile stresses acting in the plane, which are dominant in the straight segment, additional strong tangential compressive stresses act in the curved segments. With a higher blank holder force, a higher strain is expected in the flange. This leads to an increased nonuniformity with the normal pressure applied, as shown in Fig. 6b.

Material flow within flange area

To further analyze the effect of draw-in nonuniformity, an irregular speckle pattern was applied at paper blanks for the rectangular geometry. **Figure 7a** shows the displacement in the flange area at a drawing depth of 17 mm, where in the lower left corner, the calculated displacement is superimposed with the original image. For better clarity, in the top right corner, the displacement is presented solely. As can be seen by the coloring, the material flow in the flange area is nonuniform, as expected by previous findings. Individual points in the flange area can be selected and are tracked over the drawing process. Their trajectory is shown for the first 17 mm of drawing depth. At further depths, more and more of the patterns disappear due to the formation of wrinkles, leading to miscalculations and limiting the analysis. As expected, due to the tensile forces in the radial direction, the trajectories of points located in the curved segments are mostly oriented in the radial direction. In contrast, the trajectories of points in straight segments approach each other. In addition to the radial displacement component, the points also have a tangential component. The portions in x- and y-direction for the

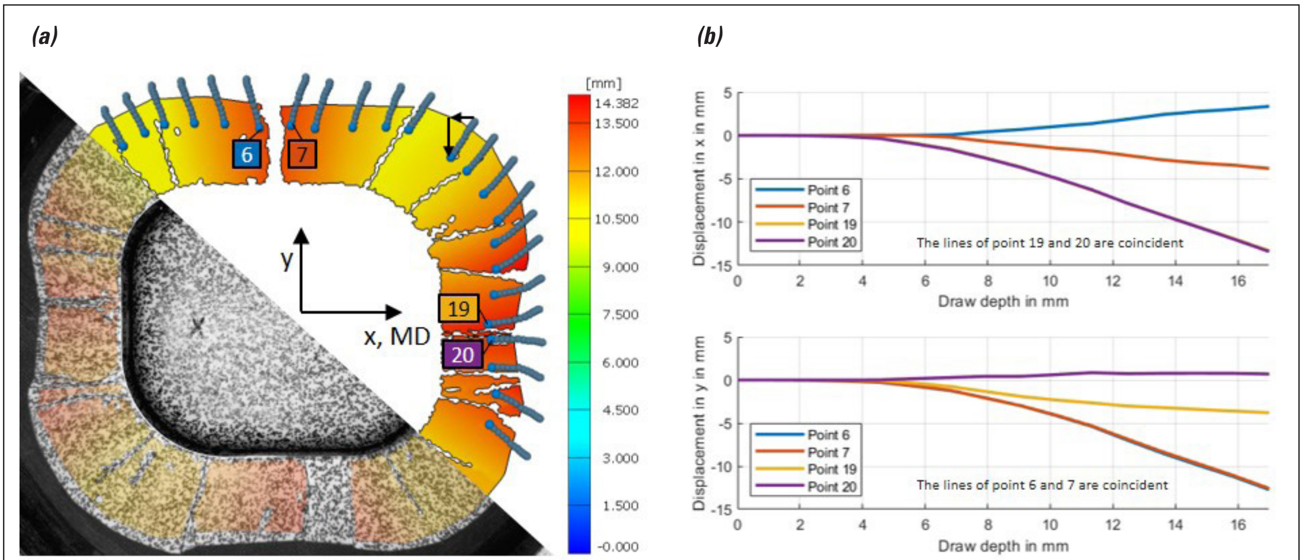

7. (a) Local material flow calculated by digital image correlation (DIC) for rectangular geometry in the flange and individual points, and (b) resulting displacements shown over drawing depth in x- and y-direction.

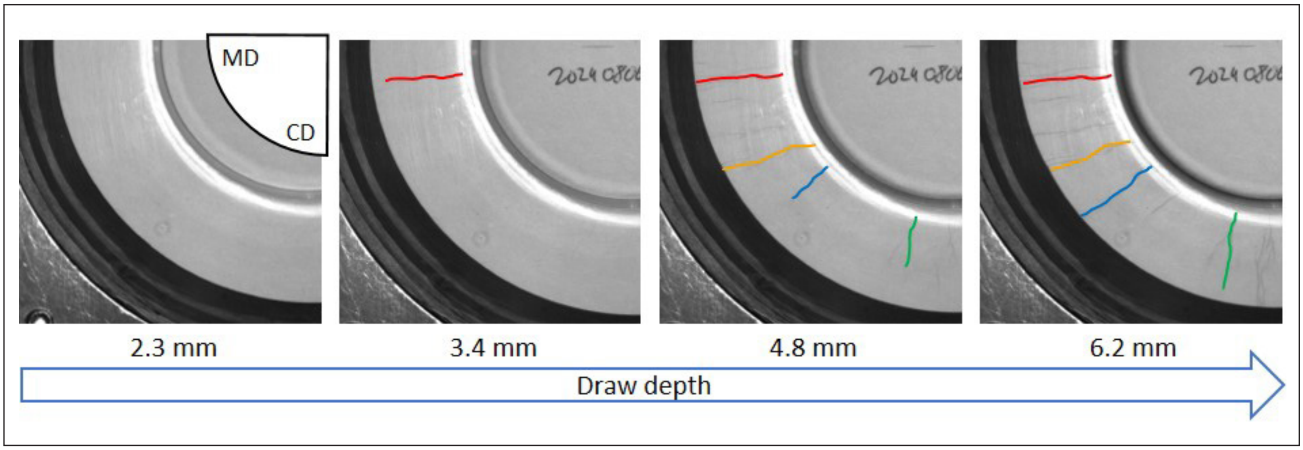

8. Formation of wrinkles as a sequence of images at different drawing depths for the round geometry.

marked points are shown in Fig. 7b. This tangential displacement leads to excess material in the straight segment, which is particularly evident at points 6 and 7, where the displacement would be expected to be close to zero, but is in the range of ± 4 mm. This excess material due to displacement results in wrinkling in segments without geometrically-caused excess material, as will be discussed in the following section.

Formation of wrinkles

Due to the die's transparency, the wrinkle formation sequence can be observed. **Figure 8** shows the wrinkle formation of a section of the flange of the round geometry as a sequence of images at different drawing depths. No wrinkles have yet formed in the flange at the first drawing depth of 2.3 mm. This is consistent with previous findings that the fiber network can absorb excess material at low drawing depths [5]. From a drawing depth of approximately 3.4 mm, at which a flange draw-in is also visible (as shown in Fig. 5), the first wrinkle (red) forms. This wrinkle is oriented along MD and spreads radially from the inside to the outside. The observed direction of propagation is intuitively contradictory to the fact that in deep drawing, the highest tangential compressive stresses occur at the outer edge of the blank due to the maximum reduction in diameter occurring there [24]. It is, therefore, hypothesized that due to the low elasticity and flowability of paperboard compared to the metals used in deep drawing, it is more appropriate to consider the instantaneous compressive stresses at infinitesimal reductions of the diameter of a circular ring disc. These are highest on the inner ring and decrease towards the outside [25]. As the process progresses, the infinitesimal displacements are expected to accumulate so that the tangential compressive stresses are highest in the outer flange area where most wrinkles occur. It must be considered that when a wrinkle is formed, the tangential compressive stresses in the immediate vicinity are reduced and influence the formation of further wrinkles in the flange.

The in-plane fibers, mainly oriented in MD, lead to a reduced perpendicular strength, simplifying the formation of wrinkles to reduce the tangential compressive stresses. As the drawing depth continues, further rising wrinkles are oriented in CD (green) and at intermediate angles (orange and blue) due to the increasing tangential compressive stresses.

In **Fig. 9**, the wrinkle formation is shown for the rectangular geometry. Similar to the first geometry, the first wrinkle appears in the convex segment with the highest tangential stresses, further developing in a radial direction towards the outside. Additionally, wrinkles in the straight segment appear as shown in the second and third images, even though no in-plane compression is expected due to material overflow [26]. Their propagation is in opposite directions, which indicates that a material displacement occurs transversely to the feed direction of the material, leading to an increase in the tangential compressive stresses in the outer flange area of the straight segment.

CONCLUSION AND OUTLOOK

The presented deep drawing setup, consisting of a transparent die and an industrial camera, enables observation of the flange during the deep drawing process. The flange draw-in can be detected and assessed as a scalar variable across the circumference, along with the material flow within the flange area and wrinkle formation. These quantities can be analyzed throughout the process, which is described by the drawing depth. It has been shown that the flange draw-in, which can be determined computationally over the drawing depth, is highly influenced by the blank-holder force, the tool geometry, and the anisotropic material behavior. At higher blank-holder forces, more strain is demanded in the flange area, resulting in longer remaining flange lengths and in higher non-uniformity for rectangular geometries. If a uniform flange length is demanded, both the material anisotropy and the process parameters must be considered when determining the blank cutting geometry.

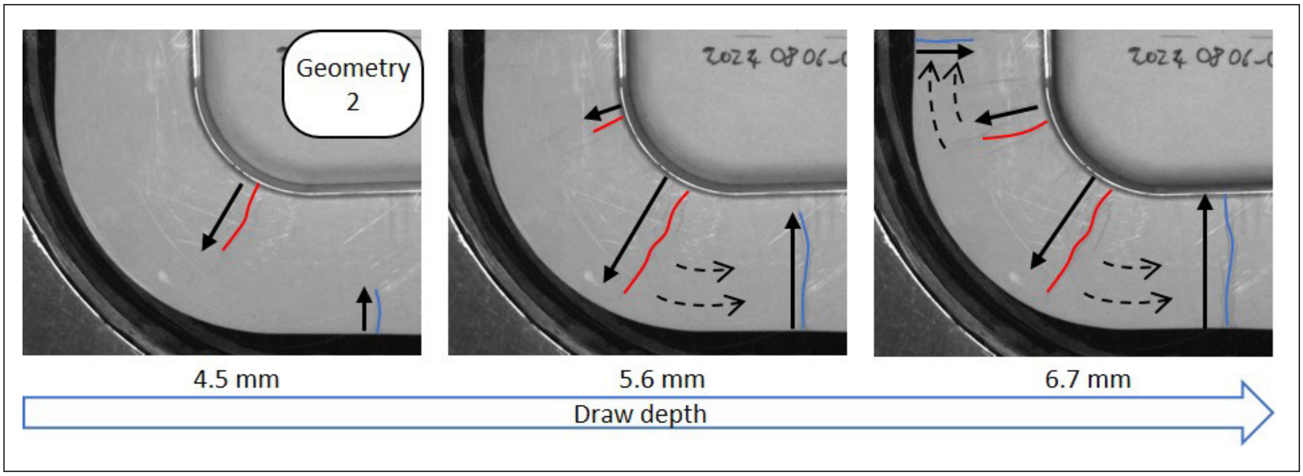

9. Formation of wrinkles (colored red and blue, with the direction of formation designated by solid arrow) as a sequence of images at different drawing depths for the rectangular geometry, and material displacement towards straight segments (designated by dashed arrows).

Analysis of the material flow within the flange area shows that there is a material redistribution from round to straight segments. Observation of the formation sequence of individual wrinkles shows the effects of this material redistribution. With the round deep-drawing geometry, the wrinkles occur in a radial direction, starting in MD and at the die feed radius. On the other hand, in the rectangular geometry, the material displacement leads to the formation of wrinkles in straight segments where there is no geometrically induced excess material. These wrinkles differ from wrinkles in the radius area by their direction of propagation, which runs from the outside to the inside.

Implementing the flange detection in the experimental setup would allow a better alignment of the paper blank before drawing, resulting in higher reproducibility of the results. To further increase the newly available options for in-depth image-based analysis, especially regarding the wrinkling behavior, further improvements are necessary. By implementing an automated wrinkle detection, a more detailed investigation of the local development and the influence of process parameters, such as the blank-holder force, is promising. Challenges for this algorithm in development are scratches, reflections, and shadows on the die, as well as the goal to detect wrinkles as early as possible in their development process. An automated wrinkle detection could then be used to improve process control, paving the way for local variations of blank-holder forces to locally influence wrinkle development. **TJ**

ACKNOWLEDGEMENT

The investigations presented in this paper were carried out within the research project DFG GR 1818/85-1 “Controlling the wrinkling of fiber-based materials through adaptive process control and camera-based data acquisition in transparent forming tools.” The authors wish to thank the German Research Foundation (DFG) for supporting the project.

LITERATURE CITED

1. Kucher, S., “Studie zeigt: Zahlungsbereitschaft für nachhaltige Verpackungen nimmt ab,” Press release, Simon-Kucher & Partners, Bonn, Germany, 6 June 2024. Available [Online] https://www.simon-kucher.com/de/wer-wir-sind/newsroom/studie-zeigt-zahlungsbereitschaft-fuer-nachhaltige-verpackungen-nimmt-ab <22Nov2024>
2. Stein, P. “Individualisierte Formgebung papierbasierter Halbzeuge,” Ph.D. thesis, Technical University of Darmstadt, Darmstadt, Germany, 2019.
3. Östlund, S., “Three-dimensional deformation and damage mechanisms in forming of advanced structures in paper,” in *Advances in Pulp and Paper Research, Oxford 2017, Trans. of the XVIth Fund. Res. Symp.* (W. Batchelor and D. Söderberg, Eds.), Oxford, 2017, pp. 489–594, FRC, Manchester, 2018. https://doi.org/10.15376/frc.2017.2.489
4. Müller, T., Lenske, A., Hauptmann, M., et al., *BioResources* 12(2): 3530(2017). https://doi.org/10.15376/biores.12.2.3530-3545.
5. Hauptmann, M., Wallmeier, M., Erhard, K., et al., *Cellulose* 22(5): 3377(2015). https://doi.org/10.1007/s10570-015-0732-x.
6. Wallmeier, M., Barbier, C., Beckmann, F., et al., *Nord. Pulp Pap. Res. J.* 36(3): 491(2021). https://doi.org/10.1515/npprj-2020-0092.
7. Tanninen, P., Leminen, V., Eskelinen, H., et al., *BioResources* 10(3): 5191(2015). https://doi.org/10.15376/biores.10.3.5191-5202.
8. Brunk, C. and Groche, P., “Influence of process parameters on the product quality in active media-based forming of paper,” in *Production at the Leading Edge of Technology, WGP 2023, Lecture Notes in Production Engineering* (T. Bauernhansl, A. Verl, M. Liewald, et al., Eds.), Springer, Cham, 2023. https://doi.org/10.1007/978-3-031-47394-4_57.
9. Hauptmann, M., Weyhe, J., and Majschak, J.-P., *J. Mater. Process. Technol.* 232: 142(2016). https://doi.org/10.1016/j.jmatprotec.2016.02.007.
10. Wallmeier, M., Linvill, E., Hauptmann, M., et al., *Mech. Mater.* 89: 202(2015). https://doi.org/10.1016/j.mechmat.2015.06.014.
11. Linvill, E., Wallmeier, M., Östlund, S., *Int. J. Solids Struct.* 117: 143(2017). https://doi.org/10.1016/j.ijsolstr.2017.03.029.

12. Jessen, N., Schetle, M., and Groche, P., "Numerical analysis of the deep drawing process of paper boards at different humidities," in *Production at the Leading Edge of Technology, WGP 2022, Lecture Notes in Production Engineering* (M. Liewald, A. Verl, T. Bauernhansl, et al., Eds.), Springer, Cham, 2023. https://doi.org/10.1007/978-3-031-18318-8_14.
13. Müller, T., Lenske, A., Barbier, C., et al., *BioResources* 14(2): 2536(2019). https://doi.org/10.15376/biores.14.2.2536-2549.
14. Wallmeier, M., Hauptmann, M., and Majschak, J.-P., *Packag. Technol. Sci.* 28(2): 91(2015). https://doi.org/10.1002/pts.2091.
15. Müller, T., Meyer, M., Lenske, A., et al., *J. Mater. Process. Technol.* 262: 615(2018). https://doi.org/10.1016/j.jmatprotec.2018.08.003.
16. Leng, Y., Sanjon, C.W., Tan, Q., et al., *J. Manuf. Mater. Process.* 8(6): 237(2024). https://doi.org/10.3390/jmmp8060237.
17. Allwood, J.M., Duncan, S.R., Cao, J., et al., *CIRP Ann.* 65(2): 573(2016). https://doi.org/10.1016/j.cirp.2016.06.002.
18. Doege, E., Seidel, H.-J., Griesbach, B., et al., *J. Mater. Process. Technol.* 130-131: 95(2002). https://doi.org/10.1016/S0924-0136(02)00763-X.
19. Rao, R.S., Devenpeck, M.L., Wright, P.K., et al., *Int. J. Mech. Sci.* 27(11-12): 725(1985). https://doi.org/10.1016/0020-7403(85)90005-0.
20. Nanao, H., Hoshi, Y., Shizuku, T., et al., *Tribol. Lett.* 60: 12(2015). https://doi.org/10.1007/s11249-015-0592-4.
21. Stora Enso, "Trayforma bleached tray board," Datasheet technical specification, Stora Enso, Helsinki. Available [Online] https://www.storaenso.com/-/media/documents/download-center/documents/product-specifications/paperboard-materials/trayforma-en.pdf <24Jan2025>

ABOUT THIS PAPER

Cite this article as:
Brunk, C. and Groche, P., *TAPPI J.* 24(8): 397(2025). https://doi.org/10.32964/TJ24.8.397

DOI: https://doi.org/10.32964/TJ24.8.397

ISSN: 0734-1415

Publisher: TAPPI Press

About this journal

22. MathWorks, "Image Processing Toolbox – MATLAB," MathWorks, Natick, MA, USA. Available [Online] https://de.mathworks.com/products/image-processing.html <03Dec2024>.
23. Vishtal, A. and Retulainen, E., *BioResources* 7(3): 4424(2012). https://doi.org/10.15376/biores.7.3.4424-4450.
24. Liewald, M., "Deep Drawing," in *CIRP Encyclopedia of Production Engineering* (S. Chatti, L. Laperrière, G. Reinhart, et al., Eds.), Springer Reference, Berlin/Heidelberg, 2019, pp. 367-371. https://doi.org/10.1007/978-3-642-20617-7_6502.
25. Mittelstedt, C., *Flächentragwerke: Scheiben, Platten, Schalen, geschichtete Strukturen*, Springer, Berlin/Heidelberg, 2022.
26. Hauptmann, M., Ehlert, S., and Majschak, J.-P., *Packag. Technol. Sci.* 27(12): 975(2014). https://doi.org/10.1002/pts.2089.

ABOUT THE AUTHORS

In this study, we present a new way of experiencing the deep drawing process of paper very directly — by making the forming zone visible. The use of a transparent die in deep drawing enables observation directly in the forming zone and throughout the entire duration of the process. This use of a transparent die supports previous investigations and assumptions on wrinkle formation and further specifies them by including the sequence.

During the study, automated detection of the flange feed over the process progress was challenging, as light reflections can lead to fault patterns. Precise positioning of the camera and light was helpful. Intensive study of flange recognition significantly expanded our understanding of automated image recognition. One surprising finding was that the direction of propagation of the wrinkles from the inside to the outside did not correspond to the expected direction.

The results of the study make it possible to better understand the process, and in particular, the formation of wrinkles. It has been shown that the blank holder force influences the forming process at a local level. Furthermore, these results pave the way for local control, as process variables can be detected with local and temporal resolution.

With additional research, findings could emerge as to which paper properties are important for good suitability for deep drawing. The next step in this research is further development of automated image analysis for the robust detection of wrinkles.

Brunk is a research associate at the Institute for Production Engineering and Forming Machines and Groche is director of the Institute and head of the Department for Functional and Composite Structures at the Technical University of Darmstadt in Darmstadt, Germany. Email Brunk at cedric.brunk@ptu.tu-darmstadt.de.

Brunk

Groche